

# A Study on the Modeling and Design of Single Phase Induction Generators

Cherl-Jin Kim<sup>†</sup> and Kwan-Yong Lee\*

**Abstract** - With increasing emphasis on non-conventional energy systems and autonomous power generation, development of improved and appropriate generating systems has recently taken on greater significance. This paper describes the performance analysis of a single phase self-excited induction generator (SEIG), suitable for autonomous/standby power systems. The system is also appropriate for wind energy systems and small portable systems. Both windings of the induction machine, the main and the auxiliary, are utilized. One winding will be devoted to the supply excitation current only, by being connected to the excitation capacitor, while the load is connected across the other winding. As the design of excitation, the minimum of self-excited capacitor connected auxiliary winding is determined as the suitable value using a circuit equation of auxiliary winding. For the steady state analysis, the equivalent circuit of the single-phase induction generators is used as a basis for modeling using the double-revolving field theory. The validity of the designed generator system is confirmed by experimental and computed results.

**Keywords:** Induction machines, Self-Excitation Induction Generator (SEIG), Single-phase Induction Generators

## 1. Introduction

In recent years, it has become increasingly necessary to improve and develop the performance of alternative energy systems such as wind power generation and independent autonomous systems by self-generation. Tremendous amounts of research have been performed on the advantages of three phase SEIGs as a general AC generation suitable for 10-100kW output range. In case of portable generation, however, the single-phase induction generator is suitable for 0.1-10kW output power.

In this study, an equivalent model of a small single-phase SEIG, design and characteristic analysis are presented. The suggested system has some advantages such as lower output requirement, cost-effectiveness, brushlessness and ease of maintenance. The proposed system has distinctive features such as the composition of auxiliary winding with parallel capacitor for self-excitation, and the load being connected with the main winding. These two windings are kept electrically at a 90° phase difference respectively.

In this paper, the steady state analysis is performed with an equivalent circuit model based on the double rotating magnetic field theory. It clarifies the suitable electric

capacitance for self-excitation, which is decided by equivalent circuit analysis and experimental results.

## 2. Characteristics of 2-Windings Self-Excited Induction Generator

### 2.1 Basic structure

Fig. 1 shows the single-phase SEIG structure suggested in this study. The generator system is composed of speed shift gears, parallel capacitors, single-phase induction generator and loads. The prime mover is used as a speed controllable induction motor, and this motor rotates together with the connected induction generator through a mechanical coupler. The SEIG is of squirrel cage type and

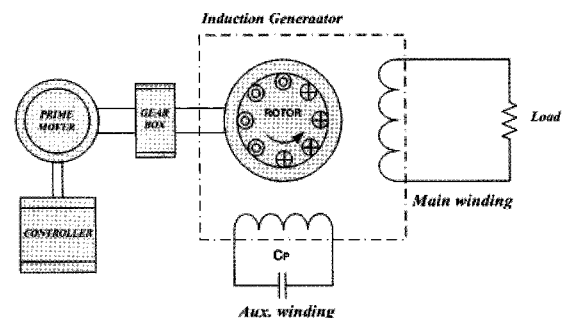


Fig. 1 Basic structure of SEIG

<sup>†</sup> Dept. of Electrical Engineering, Halla University, Korea. (cjkim@halla.ac.kr)

\* Dept. of Electrical Engineering, Halla University, Korea. (computerwin@naver.com)

has two-windings, the main and the auxiliary winding. Especially, the self-excited capacitor and resistive load are connected respectively with electrical 90 phase degrees. The excitation components caused by voltage induction of the small SEIG are composed of rotor residual magnetism and self-excitation component, which are kept in continuous energy circulation by parallel capacitor  $C_p$  connected to the auxiliary winding.

### 2.2 System Modeling

The system and equivalent circuits for analysis are modeled based on the double rotating magnetic field theory. Fig. 2 shows the steady state equivalent circuit of a two-winding SEIG. In this figure, magnetizing reactance of reverse field is very large in comparison with that of the rotator viewed in the stator, so this field can be neglected. In addition, the reactive power component of auxiliary winding supplied for field excitation can be expressed by the impedance difference between the main winding and auxiliary winding.

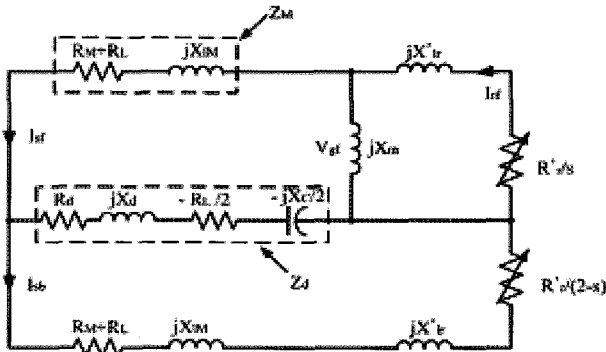


Fig. 2 SEIG equivalent circuits based on double-revolving magnetic field theory

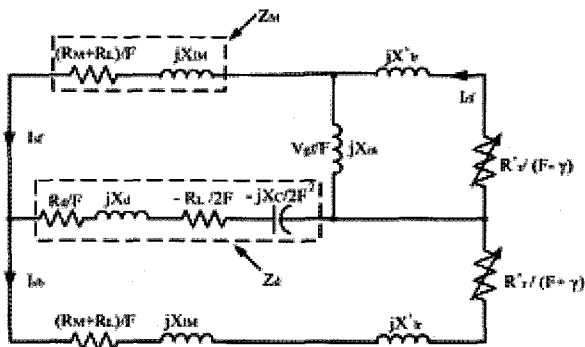


Fig. 3 Normalized equivalent circuit

The performance of a two winding SEIG can be analyzed at variable speed, so that it is available to treat the parameters measured under the rated frequency as a constant and normalizing process. So the normalized equivalent circuit can be expressed as in Fig. 3. From Fig.

3, the characteristic equations are as follows,

$$R_d = [R'_A - R_M] / 2 \tag{1}$$

$$X_d = [X'_{LA} - X_{LM}] / 2 \left( R'_A = \frac{R_A}{a^2}, X'_{LA} = \frac{X_{LA}}{a^2} \right) \tag{2}$$

$$\dot{Z}_d = R_d + jX_d - \frac{R_L}{2F} - \frac{jX_C}{2F^2} \tag{3}$$

$$\dot{Z}_M = \frac{R_M + R_L}{F} + jX_{LM} \tag{4}$$

$$\dot{I}_{sf} = \frac{V_{gf}}{F} \left( \frac{\dot{Z}_M + \dot{Z}_d + \frac{R_r}{F + \gamma} + jX_{lr}}{D} \right) \tag{5}$$

$$\dot{D} = \left[ \left( \dot{Z}_M + \dot{Z}_d \right) \left( \dot{Z}_M + \dot{Z}_d + \frac{R_r}{F + \gamma} + jX_{lr} \right) \right] - \dot{Z}_d^2 \tag{6}$$

$$\dot{I}_{sb} = V_{gf} \dot{Z}_d / D F \tag{7}$$

$$\dot{I}_{rf} = \frac{-V_{gf} / F}{\left( \frac{R_r}{F - \gamma} + jX_{lr} \right)} \tag{8}$$

$$\dot{I}_M = \dot{I}_{sf} + \dot{I}_{sb} \tag{9}$$

$$\dot{I}_A = j \left( \dot{I}_{sf} - \dot{I}_{sb} \right) \tag{10}$$

$$P_{gf} = |I_{gf}|^2 R_L, P_{gb} = |I_{gb}|^2 R_L \tag{11}$$

$$T = \frac{P_{gf} - P_{gb}}{\omega_R} \tag{12}$$

$$P_{out} = |I_M|_2 R_L \tag{13}$$

$$P_{in} = 2|I_{rf}|^2 \frac{R_r \gamma}{F - \gamma} + 2|I_{sb}|^2 \frac{R_r \gamma}{F - \gamma} \tag{14}$$

$$\eta = \frac{P_{out}}{P_{in} + P_c + P_{FW}} \tag{15}$$

All parameters of small SEIGs are calculated from experimental results and the magnetic analysis program package. Resistance and leakage reactance are produced by DC resistance measurement and a rotor locking test. Magnetizing reactance  $X_m$  is variable by air-gap magnetic flux and  $V_g$  which is changed by rotating speed. Therefore, we can find magnetizing reactance  $X_m$  from synchronous speed test, voltage  $V_g$  measurement and magnetizing performance  $I_m$ . And also we know some parameters as torque, input and output power and efficiency from Eqs. (11)-(15).

## 2.2 Selection of optimum parallel Capacitor $C_p$ for the self-excitation

Self-excitation is excited by reciprocal relation of rotor residual magnetism and self-excited capacitor. The induced current generated by the reverse field of the stator winding generates the single-direction field resulting in generator operation. When the machine is driven by an external prime mover, the current is induced in the stator winding because of residual flux of the rotator. Connection of suitable capacitors to both ends of auxiliary winding causes leading current. This current increases the core flux, and the voltage difference between induction voltage and capacitors can be constant. The continuous increasing of voltage is controlled by magnetic saturation and voltage finally reaches steady state. The stable voltage depends on speed, electric capacitance, machine parameters, magnetic characteristics and loads. Such magnetic excitation phenomena are caused by continuous energy circulation between the electric field (capacitors) and the magnetic field (machines). Also, the proper capacitance for self-excitation can be decided by the double revolving field theory. The currents of the main and auxiliary windings are separately  $i_m = \sqrt{2}I_m \cos \omega t$ ,  $i_a = \sqrt{2}I_a \cos(\omega t + \theta_a)$ . It can be expressed as;

$$\begin{aligned} F(\theta, t) &= F_m(\theta, t) + F_a(\theta, t) \\ &= \sqrt{2}N_m I_m \cos \omega t \cos \theta + \sqrt{2}N_a I_a \cos(\omega t + \theta_a) \cos(\theta + 90^\circ) \end{aligned} \quad (16)$$

Where,  $\theta_a$  is the phase difference of main and auxiliary windings and  $90^\circ$  means electric angle of geometry.

Equation (16) can be divided as forward and backward MMF.

$$\begin{aligned} F(\theta, t) &= \frac{1}{\sqrt{2}} [(N_m I_m - N_a I_a \sin \theta_a) \cos(\omega t + \theta) - (N_a I_a \cos \theta_a) \sin(\omega t + \theta)] \\ &+ \frac{1}{\sqrt{2}} [(N_m I_m + N_a I_a \sin \theta_a) \cos(\omega t - \theta) + (N_a I_a \cos \theta_a) \sin(\omega t - \theta)] \end{aligned} \quad (17)$$

In Equation (17), the first term on the right side of the equation is backward MMF and the second term is forward MMF. Also, Equation (17) may simply be the forward MMF and the backward MMF in the case of  $N_m I_m = N_a I_a$ ,  $\theta_a = 90^\circ$  is zero. Therefore, the optimum value of parallel capacitor  $C_p$  can be determined in the condition of  $N_m I_m = N_a I_a$ ,  $\theta_a = 90^\circ$ . The first condition ( $N_m I_m = N_a I_a$ ) may be expressed as impedance. Equation (17) is equal to the following;

$$N_m I_m = N_a I_a, N_m \sqrt{R_m^2 + (\omega L_m)^2} = N_a \sqrt{R_a^2 + (\omega L_a - \frac{1}{\omega C_p})^2} \quad (18)$$

We may express  $C_p$  from Equation (18) as;

$$C_p = \frac{1}{\omega \left\{ R_a + \omega L_a - \left( \frac{N_a}{N_m} \right) (R_m + \omega L_m - \sqrt{2R_m \omega L_m}) \right\}} \quad (19)$$

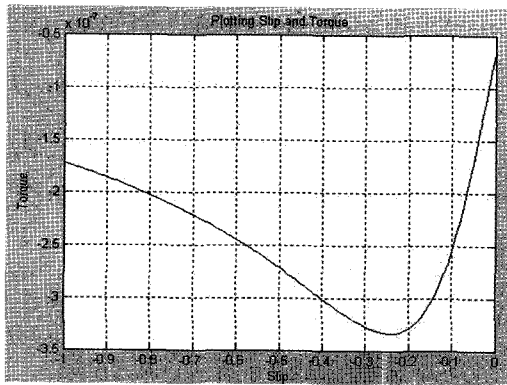
## 3. Characteristics Analysis

In order to analyze the characteristics of the single-phase induction generator, some tests are required such as DC resistance measurement, rotor locking test, and synchronous speed test.

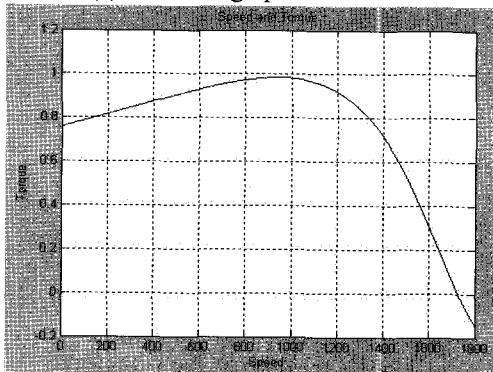
**Table 1** Parameters of single-phase induction generator

Parameters	Value
$R_M [\Omega]$	44.9
$R_A [\Omega]$	66.74
$R_r [\Omega]$	97.3
$X_{IM} [\Omega]$	21.76
$X_{IA} [\Omega]$	29.62
$X_{lr} [\Omega]$	26.95
$X_M [\Omega]$	355.03
$C_p [\mu F]$	7
$f_n [Hz]$	60
Turn ratio	1.067
$P_n [W]$	90

Magnetic analysis software package for property consideration and parameter analysis is also used. From the induced parameters, we can obtain the SEIG slip-torque characteristics using MATLAB simulations as in Fig. 4. Table I shows the parameters of the single-phase induction generator applied in this study.



(a) Generating operation mode



(b) Torque development region

Fig. 4 Slip-torque characteristics of single-phase induction motor

Fig. 4 presents the simulation results concerning slip-torque curves of the single-phase induction generator. Fig. 4(a) shows the generating operation region and Fig. 4(b) presents the torque development region of the single-phase induction motor.

#### 4. FEM Characteristics Analysis

Fig. 5 shows that the flowchart for dynamic analysis depends on the variation of time. The results of the static analysis by the finite element method were also inputted. Furthermore, it represents that the result of the necessary parameter depends on both rotor speed and time variation.

Fig. 6 represents the flux distributions of analysis model by EM-PULSE. The boundary conditions may be solved by the matrix equation of the field. The field matrix equations are as follows for stator and rotor.

$$\frac{\partial}{\partial x} \left( \frac{1}{\mu} \cdot \frac{\partial A}{\partial x} \right) + \frac{\partial}{\partial y} \left( \frac{1}{\mu} \cdot \frac{\partial A}{\partial y} \right) = J$$

$$\frac{\partial}{\partial x} \left( \frac{1}{\mu} \cdot \frac{\partial A}{\partial x} \right) + \frac{\partial}{\partial y} \left( \frac{1}{\mu} \cdot \frac{\partial A}{\partial y} \right) = \sigma \cdot \frac{\partial A}{\partial y} + J_m \quad (20)$$

Here  $A$  is zero, and the  $X$  and  $Y$  axis set up the boundary conditions. We have known that the flux exists around the pole center from the flux distributions of Fig. 6.

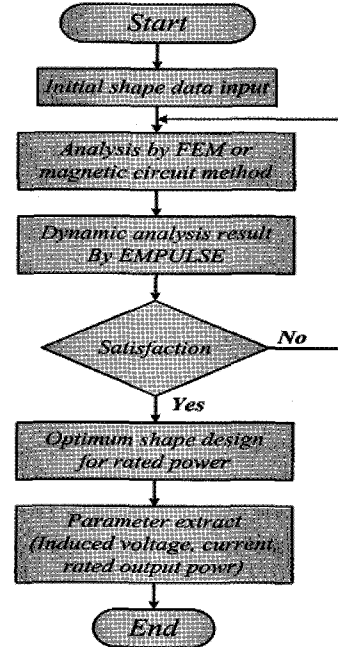


Fig. 5 Dynamic Analysis with EM-Pulse Program

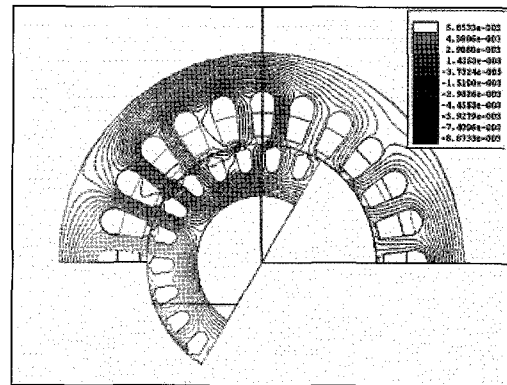


Fig. 6 Flux Distributions

#### 5. Experimental Results and Discussions

In this study, in order to estimate the characteristics of the two winding single phase SEIG, the experiment was executed using a single-phase induction motor (90[W], 4-pole,  $V_n=220[V]$ ,  $f_n=60[Hz]$ ,  $C_p=7[\mu F]$ ). The generating system consists of the prime mover, mechanical gear (ratio 1:3) and coupling device. Also by controlling the prime mover rotating speed with the controller, SEIG performance is analyzed over various speeds. Here, to analyze the SEIG performance easily and for wider speed control, we applied mechanical gear with the connected coupler.

Fig. 7 shows the experimental results which are measured across the main winding of the SEIG driven by the prime mover, while the shunt capacitor is connected across the auxiliary winding of the SEIG. Also, Fig. 7 shows capacitance-speed curves which are compared with simulation and experimental results according to the parameters of the auxiliary winding for self-excitation.

When designing the capacitance for self-excitation according to various speeds of the prime mover, we find the critical capacitance for stable self-excitation.

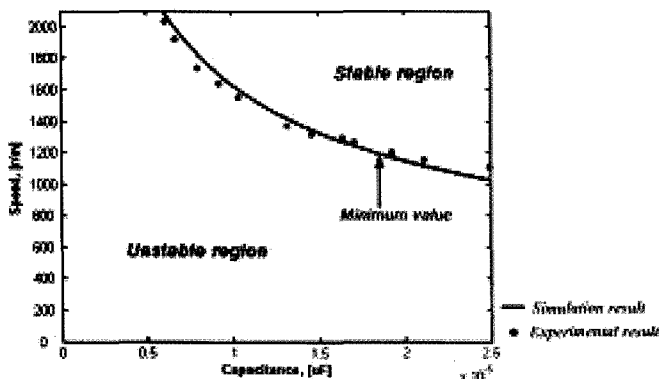


Fig. 7 Capacitance-speed characteristics

Fig. 8(a) represents no load output voltage, Fig. 8(b) shows measured output voltage and current waveforms across the load (220V/30W lamp).

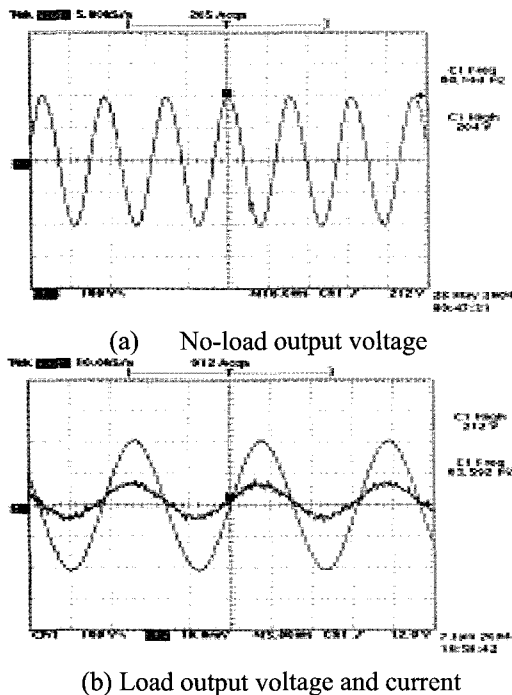


Fig. 8 Output voltage and current across the main winding

Fig. 9 represents the configuration of a single phase self-excited generating system designed and manufactured for

the experiment. In this figure, a lightening lamp is used as load.

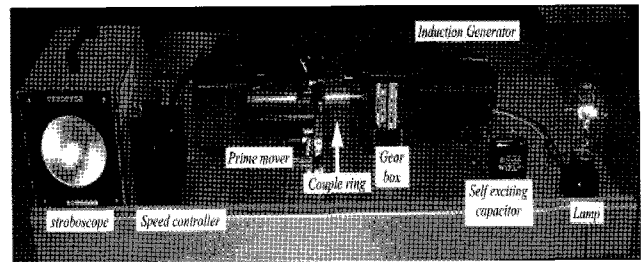


Fig. 9 Single-phase self-excited generating system

### 6. Conclusions

In this paper, the characteristic analysis and experiments of the SEIG are executed, and suitable capacitance selection of the shunt capacitor is also induced. The applied SEIG model was employed for 2-phase stator windings and cage type rotor. The shunt capacitor  $C_p$  is connected across the auxiliary winding and the load is connected across the main winding.

The required proper capacitance is to be changed depending on the various speed ranges. Consequently, the parallel capacitor selection method for self-excitation is proposed from the double-revolving field theory. From the proposal method the critical capacitance, the capacitance depending on the various speed, and the stable and unstable regions were found. The capacitor selection method and generation system was composed in order to study validity. From the experimental results, we can get good agreement between experimental and computed simulation using the Matlab results. The stable and unstable demagnetizing regions are determined clearly. In the unstable region, we found that the EMF was developed in the direction of demagnetizing the magnetic field by the residual flux density of the rotor.

Also, we confirmed that the output voltage and current had stable operation in the magnetizing direction according to the loaded experimental results.

### Acknowledgment

This work has been supported by KESRI, which is funded by MOCIE (Ministry of Commerce, Industry and Energy).

### References

[1] A. E. Fitzgerald and C. Kingsley, *Electric Machinery*, McGraw Hill Book Co. 2nd, pp. 528-538, 1961.

- [2] N. N. Hancock, *Matrix Analysis of Electric Machinery*, Pergamon, pp. 103-163 and 220, 1964.
- [3] C. G. Veinott, *Theory and Design of Small Induction Motors*, McGraw Hill Book Co., pp. 184-196 and pp. 354-364, 1959.
- [4] C. G. Veinott and J. E. Martin, *Fractional and sub-fractional Horse Power Electric Motors*, McGraw Hill Book Co., Fourth Edition Fig. 10 Photograph of the Developed SEIG.
- [5] D. B. Watson, J. Ariliaga and T. Ednsam, "Controllable d.c. power supply horn wind driven self-excited induction machines," *Proc. IEE*, vol. 126, pp. 1245-1248, Dec. 1979.

**Cherl-Jin Kim**

He received his B.S., M.S. and Ph.D. degrees in Electrical Engineering from Hanyang University, Seoul, Korea between 1980 and 1991. He was previously with the Korea Electronics Technology Institute, where he was Head Researcher of the control systems laboratory since 1991. He has been employed with Halla University since 1995 as a Professor in the Electrical Engineering Department. His research activities are in the areas of power electronics, which include electrical machine control systems and static converter design fields.

**Kwan-Yong Lee**

He received his B.S. in Electrical Engineering, from Halla University, Won-ju, Korea in 2003. He is now working toward his M.S. at the School of Electrical Engineering at the same university. His research interests are in the area of inverters, converters, with a particular interest in the design and analysis of electrical machine controllers.